



VICTORIA UNIVERSITY
MELBOURNE AUSTRALIA

Biaxially loaded high-strength concrete-filled steel tubular slender beam-columns, Part I: Multiscale simulation

This is the Accepted version of the following publication

Liang, Qing, Patel, Vipulkumar Ishvarbhai and Hadi, Muhammad NS (2012)
Biaxially loaded high-strength concrete-filled steel tubular slender beam-columns, Part I: Multiscale simulation. *Journal of Constructional Steel Research*, 75. pp. 64-71. ISSN 0143-974X

The publisher's official version can be found at
<http://www.sciencedirect.com/science/journal/0143974X/75>
Note that access to this version may require subscription.

Downloaded from VU Research Repository <https://vuir.vu.edu.au/23263/>

Biaxially loaded high-strength concrete-filled steel tubular slender beam-columns, Part I: Multiscale simulation

Qing Quan Liang^{a,*}, Vipulkumar Ishvarbhai Patel^a, Muhammad N. S. Hadi^b

^a *School of Engineering and Science, Victoria University, PO Box 14428, Melbourne, VIC 8001, Australia*

^b *School of Civil, Mining and Environmental Engineering, University of Wollongong, Wollongong, NSW 2522, Australia*

ABSTRACT

The steel tube walls of a biaxially loaded thin-walled rectangular concrete-filled steel tubular (CFST) slender beam-column may be subjected to compressive stress gradients. Local buckling of the steel tube walls under stress gradients, which significantly reduces the stiffness and strength of a CFST beam-column, needs to be considered in the inelastic analysis of the slender beam-column. Existing numerical models that do not consider local buckling effects may overestimate the ultimate strengths of thin-walled CFST slender beam-columns under biaxial loads. This paper presents a new multiscale numerical model for simulating the structural performance of biaxially loaded high-strength rectangular CFST slender beam-columns accounting for progressive local buckling, initial geometric imperfections, high strength materials and second order effects. The inelastic behavior of column cross-sections is modeled at the mesoscale level using the accurate fiber element method. Macroscale models are developed to simulate the load-deflection responses and strength envelopes of thin-walled CFST slender beam-columns. New computational

* Corresponding author. Tel.: 61 3 9919 4134; fax: +61 3 9919 4139.
E-mail address: Qing.Liang@vu.edu.au (Q. Q. Liang)

algorithms based on the Müller's method are developed to iteratively adjust the depth and orientation of the neutral axis and the curvature at the columns ends to obtain nonlinear solutions. Steel and concrete contribution ratios and strength reduction factor are proposed for evaluating the performance of CFST slender beam-columns. Computational algorithms developed are shown to be an accurate and efficient computer simulation and design tool for biaxially loaded high-strength thin-walled CFST slender beam-columns. The verification of the multiscale numerical model and parametric study are presented in a companion paper.

Keywords: Biaxial bending; Concrete-filled steel tubes; High strength materials; Local and post-local buckling; Nonlinear analysis; Slender beam-columns.

1. Introduction

High strength thin-walled rectangular concrete-filled steel tubular (CFST) slender beam-columns in composite frames may be subjected to axial load and biaxial bending. Biaxially loaded thin-walled CFST slender beam-columns with large depth-to-thickness ratios are vulnerable to local and global buckling. No numerical models have been developed for the multiscale inelastic stability analysis of biaxially loaded high strength thin-walled CFST slender beam-columns accounting for the effects of progressive local buckling of the steel tube walls under stress gradients. The difficulty is caused by the interaction between local and global buckling and biaxial bending. However, it is important to accurately predict the ultimate strength of a thin-walled CFST slender beam-column under biaxial loads because this strength is needed in the practical design. This paper addresses the important issue of multiscale simulation of high strength thin-walled rectangular CFST slender beam-columns under combined axial load and biaxial bending.

Extensive experimental investigations have been undertaken to determine the ultimate strengths of short and slender CFST columns under axial load or combined axial load and uniaxial bending [1-9]. Test results indicated that the confinement provided by the rectangular steel tube had little effect on the compressive strength of the concrete core but considerably improved its ductility. In addition, local buckling of the steel tubes was found to remarkably reduce the ultimate strength and stiffness of thin-walled CFST short columns as reported by Ge and Usami [10], Bridge and O'Shea [11], Uy [12] and Han [13]. As a result, the ultimate strengths of rectangular CFST short columns can be determined by summation of the capacities of the steel tube and concrete core, providing that local buckling effects are taken into account as shown by Liang et al. [14]. Moreover, experimental results demonstrated that the confinement effect significantly increased the compressive strength and ductility of the concrete core in circular CFST short columns. However, this confinement effect was found to reduce with increasing the column slenderness as illustrated by Knowles and Park [2] and Liang [15]. In comparisons with researches on CFST columns under axial load and uniaxial bending, experimental investigations on biaxially loaded rectangular thin-walled CFST slender beam-columns have received little attention [16-18].

Although the performance of CFST columns could be determined by experiments, they are highly expensive and time consuming. To overcome this limitation, nonlinear analysis techniques have been developed by researchers for composite columns under axial load or combined axial load and uniaxial bending [19-23]. However, only a few numerical models have been developed to predict the nonlinear inelastic behavior of slender composite columns under biaxial bending. El-Tawil et al [24] and Ei-Tawil and Deierlein [25] proposed a fiber element model for determining the inelastic moment-curvature responses and strength envelopes of concrete-encased composite columns under biaxial bending. The fiber model,

which accounted for concrete confinement effects and initial stresses caused by preloads, was used to investigate the strength and ductility of concrete-encased composite columns. A fiber element model was also developed by Muñoz and Hsu [26] that was capable of simulating the behavior of biaxially loaded concrete-encased slender composite columns. The relationship between the curvature and deflection was established by using the finite difference method. The incremental deflection approach was employed to capture the post-peak behavior of slender concrete-encased composite columns.

Lakshmi and Shanmugam [27] presented a semi-analytical model for predicting the ultimate strengths of CFST slender beam-columns under biaxial bending. An incremental-iterative numerical scheme based on the generalized displacement control method was employed in the model to solve nonlinear equilibrium equations. Extensive comparisons of computer solutions with test results were made to examine the accuracy of the semi-analytical model. However, the effects of local buckling and concrete tensile strength were not taken into account in the semi-analytical model that may overestimate the ultimate strengths of thin-walled rectangular CFST columns with large depth-to-thickness ratios. Recently, Liang [28,29] developed a numerical model based on the fiber element method for simulating the inelastic load-strain and moment-curvature responses and strength envelopes of thin-walled CFST short beam-columns under axial load and biaxial bending. The effects of local buckling were taken into account in the numerical model by using effective width formulas proposed by Liang et al. [14]. Secant method algorithms were developed to obtain nonlinear solutions. Liang [29] reported that the numerical model was shown to be an accurate and efficient computer simulation tool for biaxially loaded thin-walled normal and high strength CFST short columns with large depth-to-thickness ratios.

This paper extends the numerical models developed by Liang [21, 28] and Patel et al. [22, 23] to biaxially loaded high-strength rectangular CFST slender beam-columns with large depth-to-thickness ratios. The mesoscale model is described that determines the inelastic behavior of column cross-sections incorporating progressive local buckling. Macroscale models are established for simulating the load-deflection responses and strength envelopes of slender beam-columns under biaxial bending. New computational algorithms based on the Müller's method are developed to obtain nonlinear solutions. Steel and concrete contribution ratios and strength reduction factor are proposed for CFST slender beam-columns. The verification of the numerical model developed and its applications are given in a companion paper [30].

2. Mesoscale simulation

2.1 Fiber element model

The mesoscale model is developed by utilizing the accurate fiber element method [28] to simulate the inelastic behavior of composite cross-sections under combined axial load and biaxial bending. The rectangular CFST beam-column section is discretized into fine fiber elements as depicted in Fig. 1. Each fiber element can be assigned either steel or concrete material properties. Fiber stresses are calculated from fiber strains using the material uniaxial stress-strain relationships.

2.2 Fiber strains in biaxial bending

It is assumed that plane section remains plane under deformation. This results in a linear strain distribution throughout the depth of the section. In the numerical model, the

compressive strain is taken as positive while the tensile strain is taken as negative. Fiber strains in biaxial bending depend on the depth (d_n) and orientation (θ) of the neutral axis of the section as illustrated in Fig. 1. For $0^\circ \leq \theta < 90^\circ$, concrete and steel fiber strains can be calculated by the following equations proposed by Laing [28]:

$$y_{n,i} = \left| x_i - \frac{B}{2} \right| \tan \theta + \left(\frac{D}{2} - \frac{d_n}{\cos \theta} \right) \quad (1)$$

$$\varepsilon_i = \begin{cases} \phi |y_i - y_{n,i}| \cos \theta & \text{for } y_i \geq y_{n,i} \\ -\phi |y_i - y_{n,i}| \cos \theta & \text{for } y_i < y_{n,i} \end{cases} \quad (2)$$

in which B and D are the width and depth of the rectangular column section respectively, x_i and y_i are the coordinates of fiber i and ε_i is the strain at the i th fiber element and $y_{n,i}$ is the distance from the centroid of each fiber to the neutral axis.

When $\theta = 90^\circ$, the beam-column is subjected to uniaxial bending and fiber strains can be calculated by the following equations given by Liang [28]:

$$\varepsilon_i = \begin{cases} \phi \left| x_i - \left(\frac{B}{2} - d_n \right) \right| & \text{for } x_i \geq x_{n,i} \\ -\phi \left| x_i - \left(\frac{B}{2} - d_n \right) \right| & \text{for } x_i < x_{n,i} \end{cases} \quad (3)$$

where $x_{n,i}$ is the distance from the centroid of each fiber element to the neutral axis.

2.3 Stresses in concrete fibers

Stresses in concrete fibers are calculated from the uniaxial stress-strain relationship of concrete. A general stress-strain curve for concrete in rectangular CFST columns is shown in Fig. 2. The stress-strain curve accounts for the effect of confinement provided by the steel tube, which improves the ductility of the concrete core in a rectangular CFST column. The concrete stress from O to A in the stress-strain curve is calculated based on the equations given by Mander et al. [31] as:

$$\sigma_c = \frac{f'_{cc} \lambda \left(\frac{\varepsilon_c}{\varepsilon'_{cc}} \right)}{\lambda - 1 + \left(\frac{\varepsilon_c}{\varepsilon'_{cc}} \right)^\lambda} \quad (4)$$

$$\lambda = \frac{E_c}{E_c - \left(\frac{f'_{cc}}{\varepsilon'_{cc}} \right)} \quad (5)$$

$$E_c = 3320 \sqrt{f'_{cc}} + 6900 \quad (\text{MPa}) \quad (6)$$

in which σ_c stands for the compressive concrete stress, f'_{cc} represents the effective compressive strength of concrete, ε_c denotes the compressive concrete strain, ε'_{cc} is the strain at f'_{cc} and is between 0.002 and 0.003 depending on the effective compressive strength of concrete [28]. The Young's modulus of concrete E_c was given by ACI [32]. The effective compressive strength of concrete f'_{cc} is taken as $\gamma_c f'_c$, where γ_c is the strength reduction factor proposed by Liang [28] to account for the column size effect and is expressed by

$$\gamma_c = 1.85 D_c^{-0.135} \quad (0.85 \leq \gamma_c \leq 1.0) \quad (7)$$

where D_c is taken as the larger of $(B - 2t)$ and $(D - 2t)$ for a rectangular cross-section, and t is the thickness of the steel tube wall as shown in Fig. 1.

The parts AB, BC and CD of the stress-strain curve for concrete shown in Fig. 2 are defined by the following equations proposed by Liang [28]:

$$\sigma_c = \begin{cases} f'_{cc} & \text{for } \varepsilon'_{cc} < \varepsilon_c \leq 0.005 \\ \beta_c f'_{cc} + 100(0.015 - \varepsilon_c)(f'_{cc} - \beta_c f'_{cc}) & \text{for } 0.005 < \varepsilon_c \leq 0.015 \\ \beta_c f'_{cc} & \text{for } \varepsilon_c > 0.015 \end{cases} \quad (8)$$

where β_c was proposed by Liang [28] based on experimental results provided by Tommi and Sakino [33] to account for confinement effects on the post-peak behavior and is given by

$$\beta_c = \begin{cases} 1.0 & \text{for } \frac{B_s}{t} \leq 24 \\ 1.5 - \frac{1}{48} \frac{B_s}{t} & \text{for } 24 < \frac{B_s}{t} \leq 48 \\ 0.5 & \text{for } \frac{B_s}{t} > 48 \end{cases} \quad (9)$$

where B_s is taken as the larger of B and D for a rectangular cross-section.

The stress-strain curve for concrete in tension is shown in Fig. 2. The constitutive model assumes that the concrete tensile stress increases linearly with the tensile strain up to concrete cracking. After concrete cracking, the tensile stress of concrete decreases linearly to zero as the concrete softens. The concrete tensile stress is considered to be zero at the ultimate tensile

strain which is taken as 10 times of the strain at concrete cracking. The tensile strength of concrete is taken as $0.6\sqrt{f'_{cc}}$.

2.4 Stresses in steel fibers

Stresses in steel fibers are calculated from uniaxial stress-strain relationship of steel material. Steel tubes used in CFST cross-sections are normally made from three types of structural steels such as high strength structural steels, cold-formed steels and mild structural steels, which are considered in the numerical model. Fig. 3 shows the stress-strain relationship for three types of steels. The steel material generally follows the same stress-strain relationship under the compression and tension. The rounded part of the stress-strain curve can be defined by the equation proposed by Liang [28]. The hardening strain ε_{st} is assumed to be 0.005 for high strength and cold-formed steels and $10\varepsilon_{sy}$ for mild structure steels in the numerical model. The ultimate strain ε_{su} is taken as 0.2 for steels.

2.5 Initial local buckling

Local buckling significantly reduces the strength and stiffness of thin-walled CFST beam-columns with large depth-to-thickness ratios. Therefore, it is important to account for local buckling effects in the inelastic analysis of high strength CFST slender beam-columns. However, most of existing numerical models for thin-walled CFST beam-columns have not considered local buckling effects. This may be attributed to the complexity of the local instability problem as addressed by Liang et al. [14]. The steel tube walls of a CFST column under axial load and biaxial bending may be subjected to compressive stress gradients as depicted in Fig. 4. Due to the presence of initial geometric imperfections, no bifurcation point

can be observed on the load-deflection curves for real thin steel plates. The classical elastic local buckling theory [34] cannot be used to determine the initial local buckling stress of real steel plates with imperfections. Liang et al. [14] proposed formulas for estimating the initial local buckling stresses of thin steel plates under stress gradients by considering the effects of geometric imperfections and residual stresses. Their formulas are incorporated in the numerical model to account for initial local buckling of biaxially loaded CFST beam-columns with large depth-to-thickness ratios.

2.6. Post-local buckling

The effective width concept is commonly used to describe the post-local buckling behavior of a thin steel plate as illustrated in Fig. 4. Liang et al. [14] proposed effective width and strength formulas for determining the post-local buckling strengths of the steel tube walls of thin-walled CFST beam-columns under axial load and biaxial bending. Their formulas are incorporated in the numerical model to account for the post-local buckling effects of the steel tube walls under compressive stress gradients. The effective widths b_{e1} and b_{e2} of a steel plate under stress gradients as shown in Fig. 4 are given by Liang et al. [14] as

$$\frac{b_{e1}}{b} = \begin{cases} 0.277 + 0.01019\left(\frac{b}{t}\right) - 1.972 \times 10^{-4}\left(\frac{b}{t}\right)^2 + 9.605 \times 10^{-7}\left(\frac{b}{t}\right)^3 & \text{for } \alpha_s > 0.0 \\ 0.4186 - 0.002047\left(\frac{b}{t}\right) + 5.355 \times 10^{-5}\left(\frac{b}{t}\right)^2 - 4.685 \times 10^{-7}\left(\frac{b}{t}\right)^3 & \text{for } \alpha_s = 0.0 \end{cases} \quad (10)$$

$$\frac{b_{e2}}{b} = (2 - \alpha_s) \frac{b_{e1}}{b} \quad (11)$$

in which b is the clear width of a steel flange or web of a CFST column section, and the stress gradient coefficient $\alpha_s = \sigma_2/\sigma_1$, where σ_2 is the minimum edge stress acting on the plate and σ_1 is the maximum edge stress acting on the plate.

Liang et al. [14] suggested that the effective width of a steel plate in the nonlinear analysis can be calculated based on the maximum stress level within the steel plate using the linear interpolation method. The effective width concept implies that a steel plate attains its ultimate strength when the maximum edge stress acting on the plate reaches its yield strength. Stresses in steel fiber elements within the ineffective areas as shown in Fig. 4 are taken as zero after the maximum edge stress σ_1 reaches the initial local buckling stress σ_{1c} for a steel plate with a b/t ratio greater than 30. If the total effective width of a plate ($b_{e1} + b_{e2}$) is greater than its width (b), the effective strength formulas proposed by Liang et al. [14] are employed in the numerical model to determine the ultimate strength of the tube walls.

2.7 Stress resultants

The internal axial force and bending moments acting on a CFST beam-column section under axial load and biaxial bending are determined as stress resultants in the section as follows:

$$P = \sum_{i=1}^{ns} \sigma_{s,i} A_{s,i} + \sum_{j=1}^{nc} \sigma_{c,j} A_{c,j} \quad (12)$$

$$M_x = \sum_{i=1}^{ns} \sigma_{s,i} A_{s,i} y_i + \sum_{j=1}^{nc} \sigma_{c,j} A_{c,j} y_j \quad (13)$$

$$M_y = \sum_{i=1}^{ns} \sigma_{s,i} A_{s,i} x_i + \sum_{j=1}^{nc} \sigma_{c,j} A_{c,j} x_j \quad (14)$$

in which P stands for the axial force, M_x and M_y are the bending moments about the x and y axes, $\sigma_{s,i}$ denotes the stress of steel fiber i , $A_{s,i}$ represents the area of steel fiber i , $\sigma_{c,j}$ is the stress of concrete fiber j , $A_{c,j}$ is the area of concrete fiber j , x_i and y_i are the coordinates of steel element i , x_j and y_j stand for the coordinates of concrete element j , ns is the total number of steel fiber elements and nc is the total number of concrete fiber elements.

2.8 Inelastic moment-curvature responses

The inelastic moment-curvature responses of a CFST beam-column section can be obtained by incrementally increasing the curvature and solving for the corresponding moment value for a given axial load (P_n) applied at a fixed load angle (α). For each curvature increment, the depth of the neutral axis is iteratively adjusted for an initial orientation of the neutral axis (θ) until the force equilibrium condition is satisfied. The moments of M_x and M_y are then computed and the equilibrium condition of $\tan \alpha = M_y / M_x$ is checked. If this condition is not satisfied, the orientation of the neutral axis is adjusted and the above process is repeated until both equilibrium conditions are met. The effects of local buckling are taken into account in the calculation of the stress resultants. The depth and orientation of the neutral axis of the section can be adjusted by using the secant method algorithms developed by Liang [28] or the Müller's method [35] algorithms which are discussed in Section 4. A detailed computational procedure for predicting the inelastic moment-curvature responses of composite sections was given by Liang [28].

3. Macroscale simulation

3.1 Macroscale model for simulating load-deflection responses

The pin-ended beam-column model is schematically depicted in Fig. 5. It is assumed that the deflected shape of the slender beam-column is part of a sine wave. The lateral deflection of the beam-column can be described by the following displacement function:

$$u = u_m \sin\left(\frac{\pi z}{L}\right) \quad (15)$$

where L stands for the effective length of the beam-column and u_m is the lateral deflection at the mid-height of the beam-columns.

The curvature at the mid-height of the beam-column can be obtained as

$$\phi_m = \left(\frac{\pi}{L}\right)^2 u_m \quad (16)$$

For a beam-column subjected to an axial load at an eccentricity of e as depicted in Fig. 5 and an initial geometric imperfection u_o at the mid-height of the beam-column, the external moment at the mid-height of the beam-column can be calculated by

$$M_{me} = P(e + u_m + u_o) \quad (17)$$

To capture the complete load-deflection curve for a CFST slender beam-column under biaxial loads, the deflection control method is used in the numerical model. In the analysis, the

deflection at the mid-height u_m of the slender beam-column is gradually increased. The curvature ϕ_m at the mid-height of the beam-column can be calculated from the deflection u_m . For this curvature, the neutral axis depth and orientation are adjusted to achieve the moment equilibrium at the mid-height of the beam-column. The equilibrium state for biaxial bending requires that the following equations must be satisfied:

$$P(e + u_m + u_o) - M_{mi} = 0 \quad (18)$$

$$\tan \alpha - \frac{M_y}{M_x} = 0 \quad (19)$$

in which M_{mi} is the resultant internal moment which is calculated as $M_{mi} = \sqrt{M_x^2 + M_y^2}$.

The macroscale model incorporating the mesoscale model is implemented by a computational procedure. A computer flowchart is shown in Fig. 6 to implicitly demonstrate the computational procedure for load-deflection responses. The main steps of the computational procedure are described as follows:

- (1) Input data.
- (2) Discretize the composite section into fine fiber elements.
- (3) Initialize the mid-height deflection of the beam-column $u_m = \Delta u_m$.
- (4) Calculate the curvature ϕ_m at the mid-height of the beam-column.
- (5) Adjust the depth of the neutral axis (d_n) using the Müller's method.
- (6) Compute stress resultants P and M_{mi} considering local buckling.
- (7) Compute the residual moment $r_m^a = M_{me} - M_{mi}$.

- (8) Repeat steps (5)-(7) until $|r_m^a| < \varepsilon_k$.
- (9) Compute bending moments M_x and M_y .
- (10) Adjust the orientation of the neutral axis (θ) using the Müller's method.
- (11) Calculate the residual moment $r_m^b = \tan \alpha - \frac{M_y}{M_x}$.
- (12) Repeat steps (5)-(11) until $|r_m^b| < \varepsilon_k$.
- (13) Increase the deflection at the mid-height of the beam-column by $u_m = u_m + \Delta u_m$.
- (14) Repeat steps (4)-(13) until the ultimate axial load P_n is obtained or the deflection limit is reached.
- (15) Plot the load-deflection curve.

In the above procedure, ε_k is the convergence tolerance and taken as 10^{-4} in the numerical analysis.

3.2 Macroscale model for simulating strength envelopes

In design practice, it is required to check for the design capacities of CFST slender beam-columns under design actions such as the design axial force and bending moments, which have been determined from structural analysis. For this design purpose, the axial load-moment strength interaction curves (strength envelopes) need to be developed for the beam-columns. For a given axial load applied (P_n) at a fixed load angle (α), the ultimate bending strength of a slender beam-column is determined as the maximum moment that can be applied to the column ends. The moment equilibrium is maintained at the mid-height of the beam-column. The external moment at the mid-height of the slender beam-column is given by

$$M_{me} = M_e + P_n (u_m + u_o) \quad (20)$$

in which M_e is the moment at the column ends. The deflection at the mid-height of the slender beam-column can be calculated from the curvature as

$$u_m = \left(\frac{L}{\pi} \right)^2 \phi_m \quad (21)$$

To generate the strength envelope, the curvature (ϕ_m) at the mid-height of the beam-column is gradually increased. For each curvature increment, the corresponding internal moment capacity (M_{mi}) is computed by the inelastic moment-curvature responses discussed in Section 2.8. The curvature at the column ends (ϕ_e) is adjusted and the corresponding moment at the column ends is calculated until the maximum moment at the column ends is obtained. The axial load is increased and the strength envelope can be generated by repeating the above process. For a CFST slender beam-column under combined axial load and bending, the following equilibrium equations must be satisfied:

$$P_n - P = 0 \quad (22)$$

$$\tan \alpha - \frac{M_y}{M_x} = 0 \quad (23)$$

$$M_e + P_n (u_m + u_o) - M_{mi} = 0 \quad (24)$$

Fig. 7 shows a computer flowchart that implicitly illustrates the computational procedure for developing the strength envelope. The main steps of the computational procedure are described as follows:

- (1) Input data.
- (2) Discretize the composite section into fine fiber elements.
- (3) The load-deflection analysis procedure is used to compute the ultimate axial load P_{oa} of the axially loaded slender beam-column with local buckling effects.
- (4) Initialize the applied axial load $P_n = 0$.
- (5) Initialize the curvature at the mid-height of the beam-column $\phi_m = \Delta\phi_m$.
- (6) Compute the mid-height deflection u_m from the curvature ϕ_m .
- (7) Adjust the depth of the neutral axis (d_n) using the Müller's method.
- (8) Calculate resultant force P considering local buckling.
- (9) Compute the residual force $r_m^c = P_n - P$.
- (10) Repeat steps (7)-(9) until $|r_m^c| < \varepsilon_k$.
- (11) Compute bending moment M_x and M_y .
- (12) Adjust the orientation of the neutral axis (θ) using the Müller's method.
- (13) Calculate the residual moment $r_m^b = \tan \alpha - \frac{M_y}{M_x}$.
- (14) Repeat steps (7)-(13) until $|r_m^b| < \varepsilon_k$.
- (15) Compute the internal resultant moment M_{mi} .
- (16) Adjust the curvature at the column end ϕ_e using the Müller's method.
- (17) Compute the moment M_e at the column ends accounting for local buckling effects.
- (18) Compute $r_m^a = M_{me} - M_{mi}$.
- (19) Repeat steps (16)-(18) until $|r_m^a| < \varepsilon_k$.
- (20) Increase the curvature at the mid-height of the beam-column by $\phi_m = \phi_m + \Delta\phi_m$.

- (21) Repeat steps (6)-(20) until the ultimate bending strength $M_n (= M_{e_{\max}})$ at the column ends is obtained.
- (22) Increase the axial load by $P_n = P_n + \Delta P_n$, where $\Delta P_n = P_{oa} / 10$.
- (23) Repeat steps (5)-(22) until the maximum load increment is reached.
- (24) Plot the axial load-moment interaction diagram.

4. Numerical solution scheme

4.1 General

As discussed in the preceding sections, the depth and orientation of the neutral axis and the curvature at the column ends need to be iteratively adjusted to satisfy the force and moment equilibrium conditions in the inelastic analysis of a slender beam-column. For this purpose, computational algorithms based on the secant method have been developed by Liang [21, 28]. Although the secant method algorithms are shown to be efficient and reliable for obtaining converged solutions, computational algorithms based on the Müller's method [35], which is a generalization of the secant method, are developed in the present study to determine the true depth and orientation of the neutral axis and the curvature at the column ends.

4.2 The Müller's method

In general, the depth (d_n) and orientation (θ) of the neutral axis and the curvature (ϕ_e) at the column ends of a slender beam-column are design variables which are denoted herein by ω . The Müller's method requires three starting values of the design variables ω_1 , ω_2 , and ω_3 . The corresponding force or moment functions $r_{m,1}$, $r_{m,2}$ and $r_{m,3}$ are calculated based on the

three initial design variables. The new design variable ω_4 that approaches the true value is determined by the following equations:

$$\omega_4 = \omega_3 + \frac{-2c_m}{b_m \pm \sqrt{b_m^2 - 4a_m c_m}} \quad (25)$$

$$a_m = \frac{(\omega_2 - \omega_3)(r_{m,1} - r_{m,3}) - (\omega_1 - \omega_3)(r_{m,2} - r_{m,3})}{(\omega_1 - \omega_2)(\omega_1 - \omega_3)(\omega_2 - \omega_3)} \quad (26)$$

$$b_m = \frac{(\omega_1 - \omega_3)^2 (r_{m,2} - r_{m,3}) - (\omega_2 - \omega_3)^2 (r_{m,1} - r_{m,3})}{(\omega_1 - \omega_2)(\omega_1 - \omega_3)(\omega_2 - \omega_3)} \quad (27)$$

$$c_m = r_{m,3} \quad (28)$$

When adjusting the neutral axis depth and orientation, the sign of the square root term in the denominator of Eq. (25) is taken to be the same as that of b_m . However, this sign is taken as positive when adjusting the curvature at the column ends. In order to obtain converged solutions, the values of ω_1 , ω_2 and ω_3 and corresponding residual forces or moments $r_{m,1}$, $r_{m,2}$ and $r_{m,3}$ need to be exchanged as discussed by Patel et al. [22]. Eq. (25) and the exchange of design variables and force or moment functions are executed iteratively until the convergence criterion of $|r_m| < \varepsilon_k$ is satisfied.

In the numerical model, three initial values of the neutral axis depth $d_{n,1}$, $d_{n,3}$ and $d_{n,2}$ are taken as $D/4$, D and $(d_{n,1} + d_{n,3})/2$ respectively; the orientations of the neutral axis θ_1 , θ_3 and θ_2 are initialized to $\alpha/4$, α and $(\theta_1 + \theta_3)/2$ respectively; and the curvature at the column ends $\phi_{e,1}$, $\phi_{e,3}$ and $\phi_{e,2}$ are initialized to 10^{-10} , 10^{-6} and $(\phi_{e,1} + \phi_{e,3})/2$ respectively.

5. Performance indices for CFST slender beam-columns

Performance indices are used to evaluate the contributions of the concrete and steel components to the ultimate strengths of CFST slender beam-columns and to quantify the strength reduction caused by the section and column slenderness, loading eccentricity and initial geometric imperfections. These performance indices can be used to investigate the cost effective designs of CFST slender beam-columns under biaxial loads.

5.1 Steel contribution ratio (ξ_s)

The steel contribution ratio is used to determine the contribution of the hollow steel tubular beam-column to the ultimate strength of the CFST slender beam-column under axial load and biaxial bending, which is given by

$$\xi_s = \frac{P_s}{P_n} \quad (29)$$

where P_n is the ultimate axial strength of the CFST slender beam-column and P_s is the ultimate axial strength of the hollow steel tubular beam-column, which is calculated by setting the concrete compressive strength f'_c to zero in the numerical analysis while other conditions of the hollow steel tubular beam-column remain the same as those of the CFST beam-column. The effects of local buckling are taken into account in the determination of both P_n and P_s .

5.2 Concrete contribution ratio (ξ_c)

The concrete contribution ratio quantifies the contribution of the concrete component to the ultimate axial strength of a CFST slender beam-column. The slender concrete core beam-column without reinforcement carries very low loading and does not represent the concrete core in a CFST slender beam-column. Portolés et al. [9] used the capacity of the hollow steel tubular beam-column to define the concrete contribution ratio (CCR), which is given by

$$\text{CCR} = \frac{P_n}{P_s} \quad (30)$$

Eq. (30) is an inverse of the steel contribution ratio and may not accurately quantify the concrete contribution. To evaluate the contribution of the concrete component to the ultimate axial strength of a CFST slender beam-column, a new concrete contribution ratio is proposed as

$$\xi_c = \frac{P_n - P_s}{P_n} \quad (31)$$

It can be seen from Eq. (31) that the concrete contribution to the ultimate axial strength of a CFST slender beam-column is the difference between the ultimate axial strength of the CFST column and that of the hollow steel column.

5.3 Strength reduction factor (α_c)

The ultimate axial strength of a CFST short column under axial loading is reduced by increasing the section and column slenderness, loading eccentricity, and initial geometric imperfections. To reflect on these effects, the strength reduction factor is defined as

$$\alpha_c = \frac{P_n}{P_o} \quad (32)$$

where P_o is the ultimate axial strength of the column cross-section under axial compression. The ultimate axial strengths of P_n and P_o are determined by considering the effects of local buckling of the steel tubes.

6. Conclusions

This paper has presented a new multiscale numerical model for the nonlinear inelastic analysis of high strength thin-walled rectangular CFST slender beam-columns under combined axial load and biaxial bending. At the mesoscale level, the inelastic axial load-strain and moment-curvature responses of column cross-sections subjected to biaxial loads are modeled using the accurate fiber element method, which accounts for the effects of progressive local buckling of the steel tube walls under stress gradients. Macroscale models together with computational procedures have been described that simulate the axial load-deflection responses and strength envelopes of CFST slender beam-columns under biaxial bending. Initial geometric imperfections and second order effects between axial load and deformations are taken into account in the macroscale models. New solution algorithms based on the Müller's method have been developed and implemented in the numerical model to obtain converged solutions.

The computer program that implements the multiscale numerical model developed is an efficient and powerful computer simulation and design tool that can be used to determine the structural performance of biaxially loaded high strength rectangular CFST slender beam-

columns made of compact, non-compact or slender steel sections. This overcomes the limitations of experiments which are extremely expensive and time consuming. Moreover, the multiscale numerical model can be implemented in frame analysis programs for the nonlinear analysis of composite frames. Steel and concrete contribution ratios and strength reduction factor proposed can be used to study the optimal designs of high strength CFST beam-columns. The verification of the numerical model and parametric study are given in a companion paper [30].

References

- [1] Furlong RW. Strength of steel-encased concrete beam-columns. *Journal of the Structural Division, ASCE* 1967; 93(5):113-24.
- [2] Knowles RB, Park R. Strength of concrete-filled steel tubular columns. *Journal of Structural Divisions, ASCE* 1969; 95(12):2565-87.
- [3] Schneider SP. Axially loaded concrete-filled steel tubes. *Journal of Structural Engineering, ASCE* 1998; 124(10):1125-38.
- [4] Varma AH, Ricles JM, Sause R, Lu LW. Seismic behavior and modeling of high-strength composite concrete-filled steel tube (CFT) beam-columns. *Journal of Constructional Steel Research* 2002; 58:725–58.
- [5] Sakino K, Nakahara H, Morino S, Nishiyama I. Behavior of centrally loaded concrete-filled steel-tube short columns. *Journal of Structural Engineering, ASCE* 2004; 130(2):180-88.
- [6] Fujimoto T, Mukai A, Nishiyama I, Sakino K. Behavior of eccentrically loaded concrete-filled steel tubular columns. *Journal of Structural Engineering, ASCE* 2004;130(2):203-12.

- [7] Ellobody E, Young B, Lam D. Behaviour of normal and high strength concrete-filled compact steel tube circular stub columns. *Journal of Constructional Steel research* 2006; 62(7): 706-15.
- [8] Liu D. Behaviour of eccentrically loaded high-strength rectangular concrete-filled steel tubular columns. *Journal of Constructional Steel Research* 2006; 62(8): 839-46.
- [9] Portolés JM, Romero ML, Bonet JL, Filippou FC. Experimental study on high strength concrete-filled circular tubular columns under eccentric loading. *Journal of Constructional Steel Research* 2011; 67(4): 623-33
- [10] Ge HB, Usami T. Strength of concrete-filled thin-walled steel box columns: Experiment. *Journal of Structural Engineering, ASCE* 1992; 118(11):3036-54.
- [11] Bridge RQ, O'Shea MD. Behaviour of thin-walled steel box sections with or without internal restraint. *Journal of Constructional Steel Research* 1998; 47(1-2):73-91.
- [12] Uy B. Strength of concrete filled steel box columns incorporating local buckling. *Journal of Structural Engineering, ASCE* 2000; 126(3):341-52.
- [13] Han LH. Tests on stub columns of concrete-filled RHS sections. *Journal of Constructional Steel research* 2002; 58(3):353-72.
- [14] Liang QQ, Uy B, Liew JYR. Local buckling of steel plates in concrete-filled thin-walled steel tubular beam-columns. *Journal of Constructional Steel Research* 2007; 63(3):396-405.
- [15] Liang QQ. High strength circular concrete-filled steel tubular slender beam-columns, Part II: Fundamental behavior. *Journal of Constructional Steel Research* 2011; 67(2): 172-180.
- [16] Bridge RQ. Concrete filled steel tubular columns. School of Civil Engineering, The University of Sydney, Sydney, Australia, Research Report No. R 283, 1976.

- [17] Shakir-Khalil H, Zeghiche J. Experimental behaviour of concrete-filled rolled rectangular hollow-section columns. *The structural Engineer*, 1989; 67(19): 346-53.
- [18] Shakir-Khalil H, Mouli M. Further tests on concrete-filled rectangular hollow-section columns. *The structural Engineer*, 1990; 68(20):405-413.
- [19] Vrcelj Z, Uy B. Strength of slender concrete-filled steel box columns incorporating local buckling. *Journal of Constructional Steel research* 2002; 58(2):275-300.
- [20] Hu HT, Huang CS, Wu MH, Wu YM. Nonlinear analysis of axially loaded concrete-filled tube columns with confinement effect. *Journal of Structural Engineering, ASCE* 2003; 129(10): 1322-29.
- [21] Liang QQ. High strength circular concrete-filled steel tubular slender beam-columns, Part I: Numerical analysis. *Journal of Constructional Steel Research* 2011; 67(2): 164-171.
- [22] Patel VI, Liang QQ, Hadi MNS. High strength thin-walled rectangular concrete-filled steel tubular slender beam-columns, Part I: Modeling. *Journal of Constructional Steel Research* 2012; 70: 377-384.
- [23] Patel VI, Liang QQ, Hadi MNS. High strength thin-walled rectangular concrete-filled steel tubular slender beam-columns, Part II: Behavior. *Journal of Constructional Steel Research* 2012; 70: 368-376.
- [24] El-Tawil S, Sanz-Picon CF, Deierlein GG. Evaluation of ACI 318 and AISC (LRFD) strength provisions for composite beam-columns. *Journal of Constructional Steel Research* 1995; 34(1):103-23.
- [25] El-Tawil S and Deierlein GG. Strength and ductility of concrete encased composite column. *Journal of Structural Engineering* 1999; 125(9): 1009-19.
- [26] Muñoz, PR, Hsu CTT. Behavior of biaxially loaded concrete-encased composite columns. *Journal of Structural Engineering, ASCE* 1997; 123(9): 1183-1171.

- [27] Lakshmi B, Shanmugam NE. Nonlinear analysis of in-filled steel-concrete composite columns. *Journal of Structural Engineering, ASCE* 2002; 128(7):922-33.
- [28] Liang QQ. Performance-based analysis of concrete-filled steel tubular beam-columns, Part I: Theory and algorithms. *Journal of Constructional Steel Research* 2009; 65(2):363-72.
- [29] Liang QQ. Performance-based analysis of concrete-filled steel tubular beam-columns, Part II: Verification and applications. *Journal of Constructional Steel Research* 2009; 65(2):351-62.
- [30] Patel VI, Liang QQ, Hadi MNS. Biaxially loaded high-strength concrete-filled steel tubular slender beam-columns, Part II: Parametric study. *Journal of Constructional Steel Research* 2014 (in press).
- [31] Mander JB, Priestley MJN, Park R. Theoretical stress-strain model for confined concrete. *Journal of Structural Engineering, ASCE* 1988; 114(8):1804-26.
- [32] ACI-318. *Building Code Requirements for Reinforced Concrete*. ACI, Detroit, MI, 2002.
- [33] Tomii M, Sakino K. Elastic-plastic behavior of concrete filled square steel tubular beam-columns. *Transactions of the Architectural Institute of Japan* 1979;280:111-20.
- [34] Bulson PS. *The stability of flat plates*. Chatto and Windus, London, 1970.
- [35] Müller DE. A method for solving algebraic equations using an automatic computer. *MTAC*, 1956, 10:208-15.

Figures

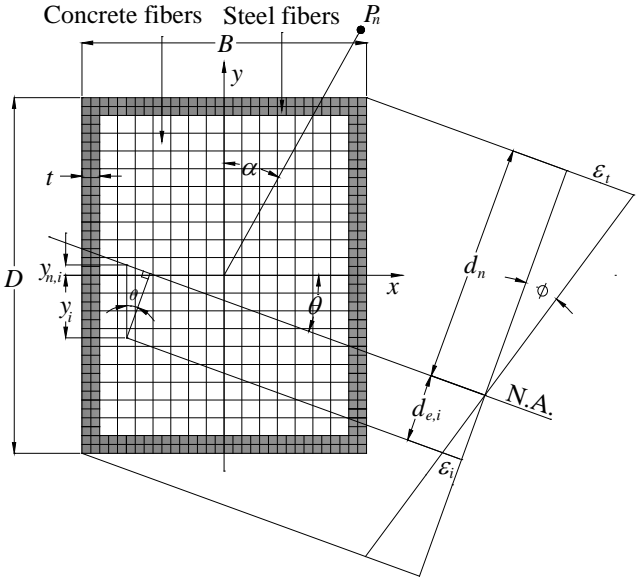


Fig. 1. Fiber element discretization and strain distribution of CFST beam-column section.

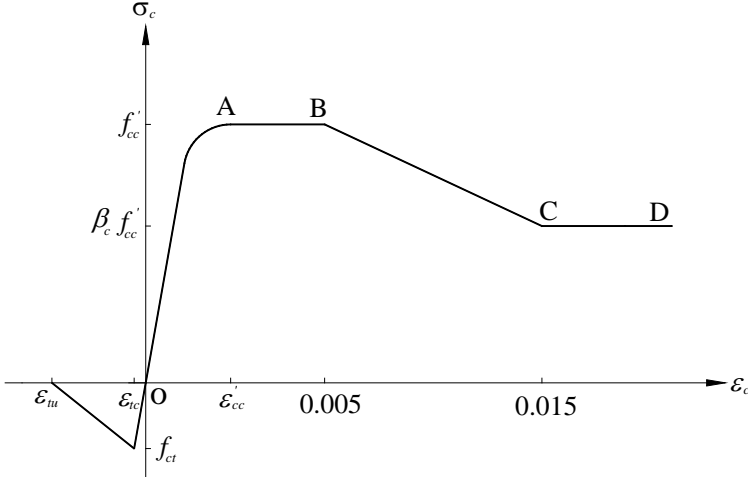


Fig. 2. Stress-strain curve for confined concrete in rectangular CFST columns.

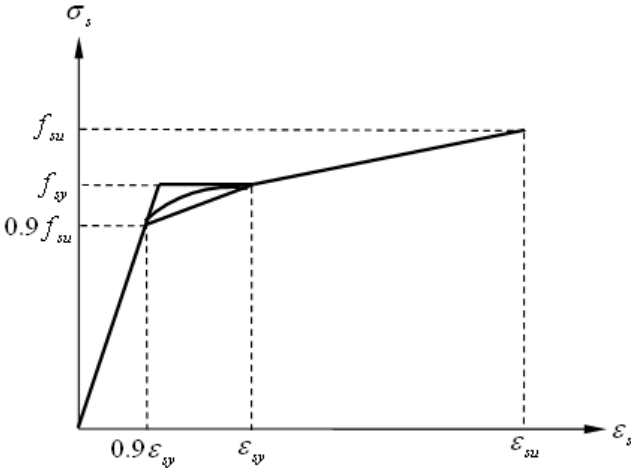


Fig. 3. Stress-strain curves for structural steels.

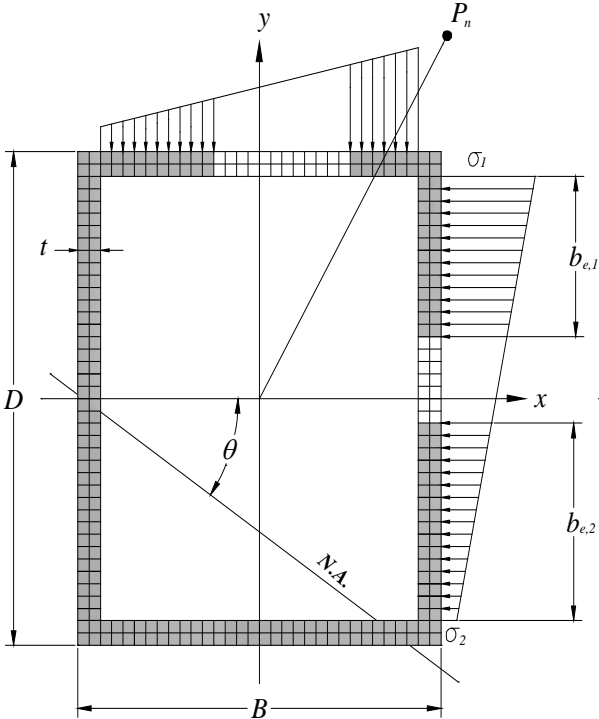


Fig. 4. Effective and ineffective areas of steel tubular cross-section under axial load and biaxial bending.

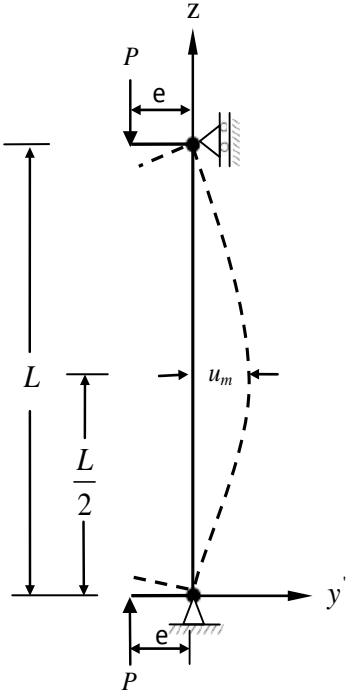


Fig. 5. Pin-ended beam-column model.

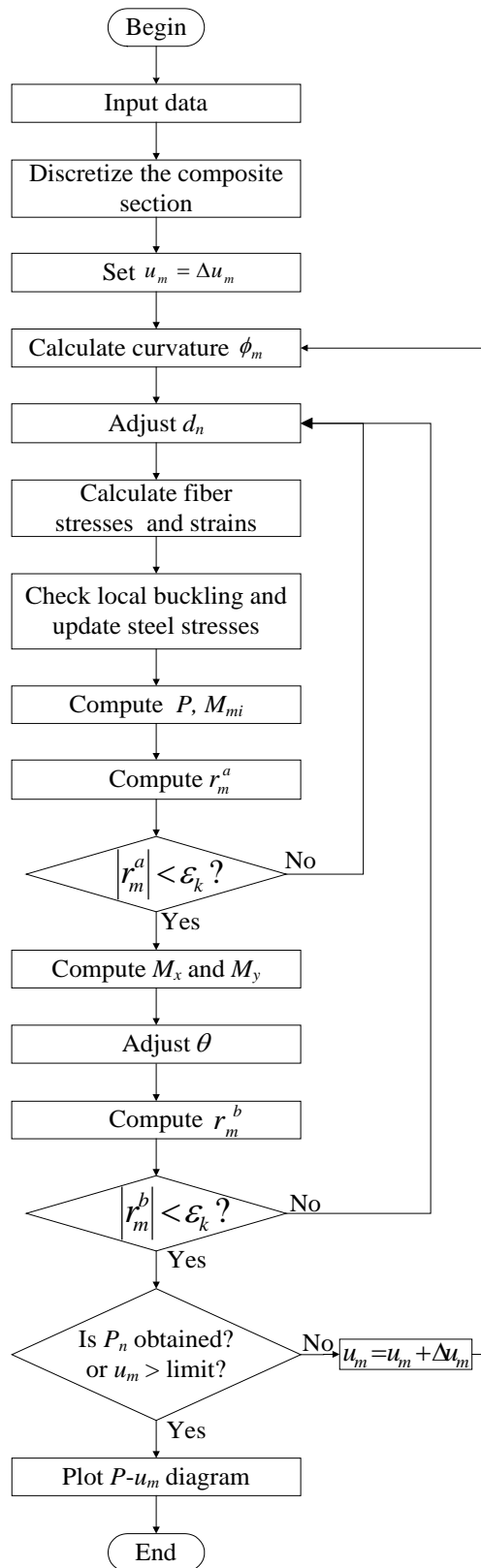


Fig. 6. Computer flowchart for predicting the axial load-deflection responses of thin-walled CFST slender beam-columns under biaxial loads

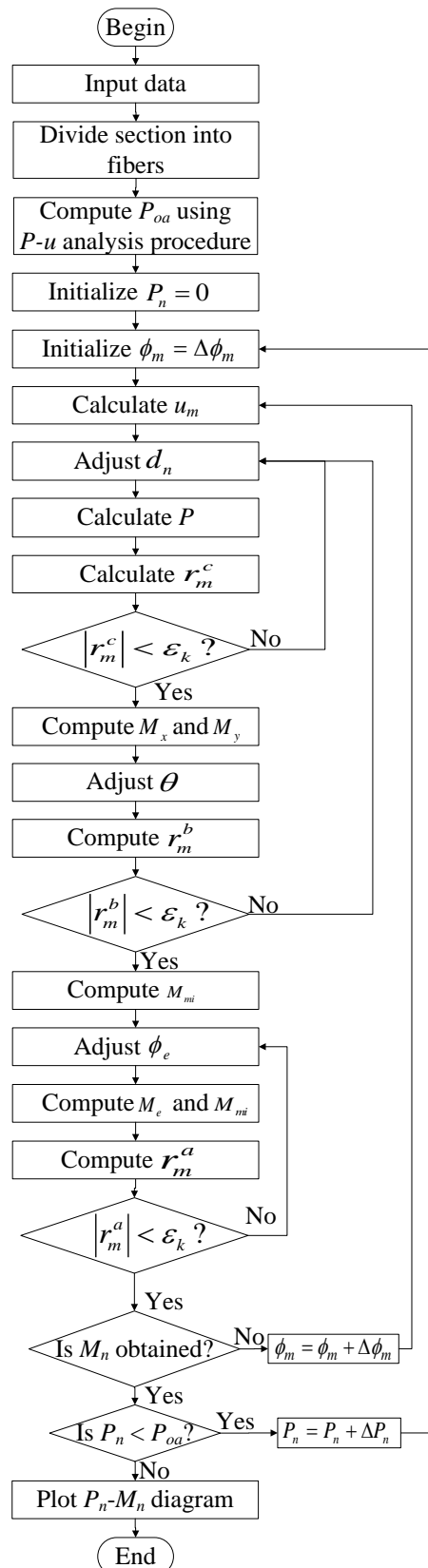


Fig. 7. Computer flowchart for simulating the strength envelopes of thin-walled CFST slender beam-columns under biaxial loads